IsoCamp
SIRFER @ Utah
2017
stableisotopes.utah.edu

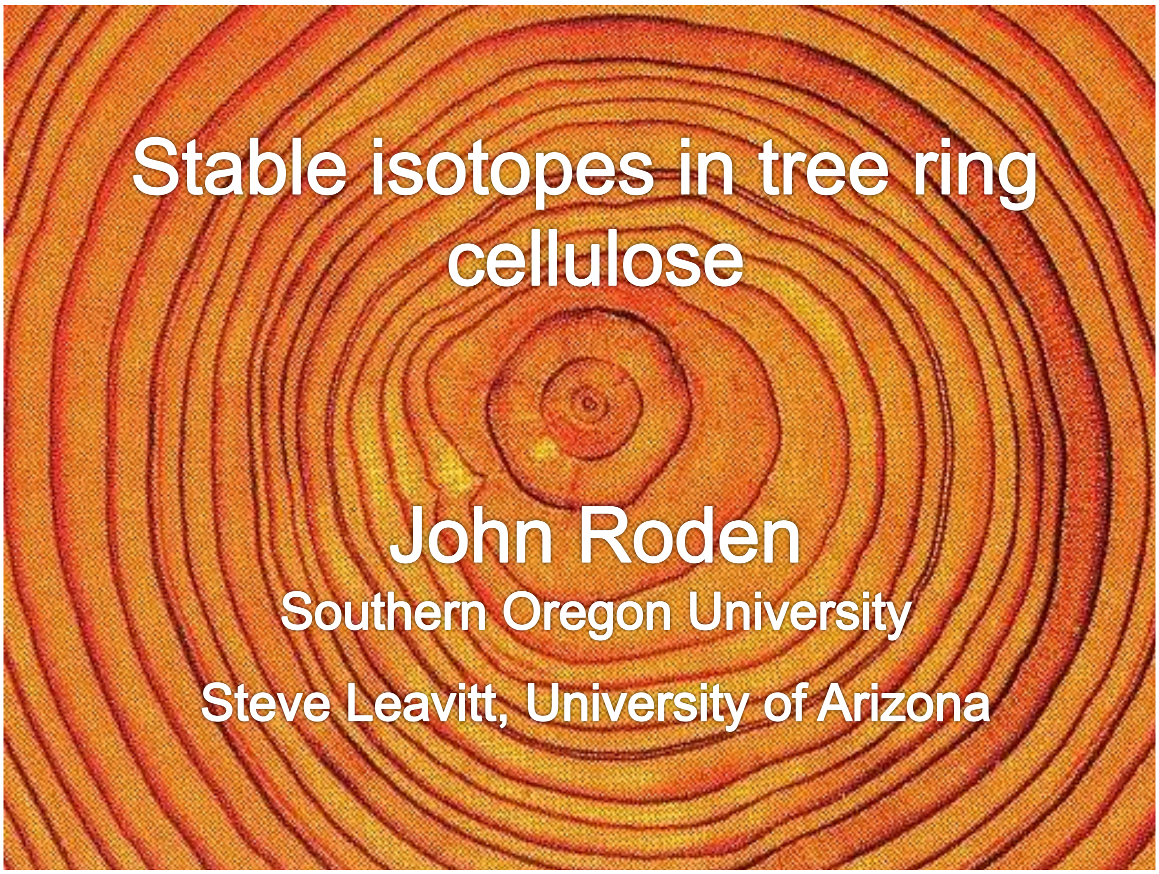

Stable isotopes in tree ring cellulose

John Roden

Southern Oregon University

Outline

- Introduction – tree ring basics & cross-dating
- Tree ring sampling and processing
- Sources of isotopes in organic matter and analysis
- Modeling stable isotope variation in organic matter
- Causes of isotope variation in organic matter
- Case studies and future directions.

Anatomy of Growth Rings

Terminology

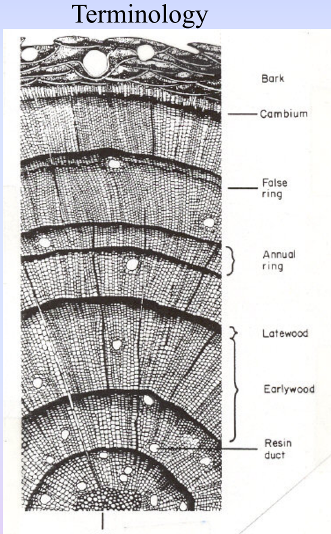

Conifer
"non-porous"

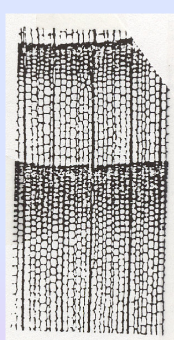

"ring-porous"

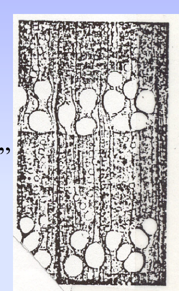

Angiosperms

"diffuse-porous"

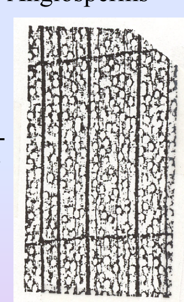

Plant components, approximate % dry weight and relative tissue decomposition rate

Plant component	% dry weight	General Composition	Relative Decomposition*
Carbohydrates		CHO	
Sugars, Starches	1-5		1
Hemicelluloses	10-30		4
Cellulose	20-50		5
Proteins		CHONPS	
simple H_2O-soluble			2
conjugated			3
Lignins	10-30	CHO	6
Lipids	1-8	CHO	7

* 1-7, Highest to Lowest

"Sensitive" and "Complacent" Tree-Ring Chronologies

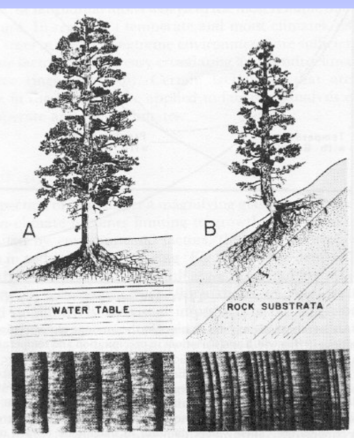

FIG. 1.5. Trees growing on sites where climate seldom limits growth processes produce rings that are uniformly wide (A). The ring widths provide little or no record of variations in climate and are termed *complacent*. Trees growing on sites where climatic factors are frequently limiting produce rings that vary in width from year to year depending upon how severely limiting climate has been to growth (B). These are termed *sensitive*.

(Fritts 1976)

But stable isotopes can provide valuable climate information even on complacent sites (see Hartl-Meier et al., 2015; Cernusak and English 2015).

Developing Tree-Ring Chronologies

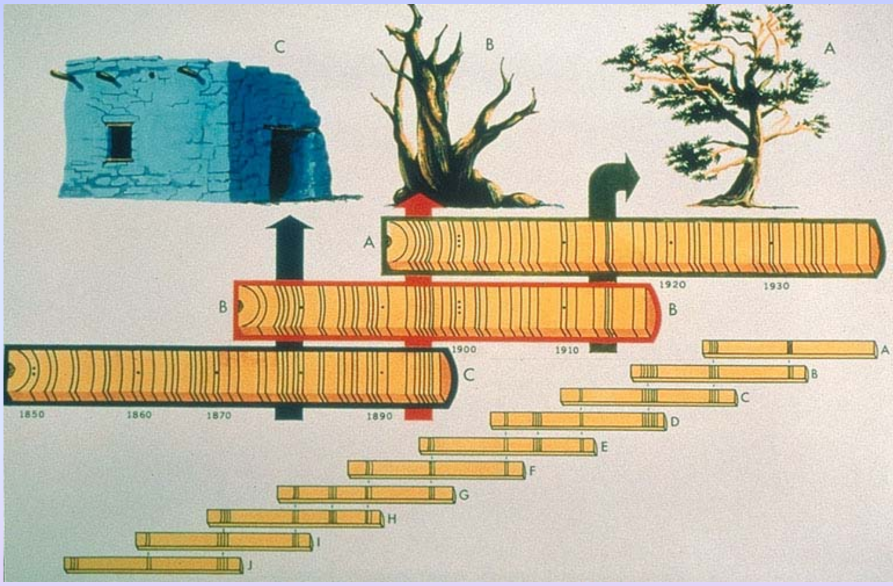

Cross-sections ("disks" or "cookies") may be particularly useful in some circumstances,

eg, (1) a lot of material is needed,
(2) new species with unknown characteristics,
(3) species with reputation for problems.

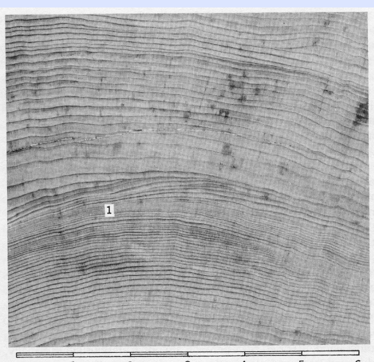

Figure 1-3 Discontinuous rings (above 1) in redwood [*Sequoia sempervirens* (D. Don) Endl.]. (*Photograph by E. Fritz.*)

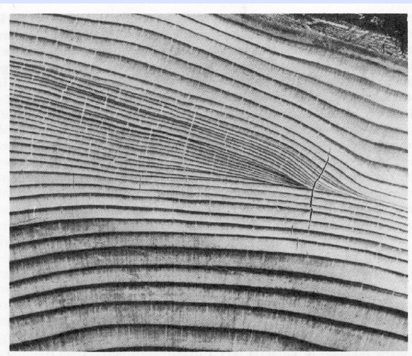

FIG. 2.28. A cross section from a coniferous stem with 18 growth rings absent on the right side of the photograph but present on the left. (Photo by James Harsha)

Tree-Ring Chronologies Around the World, ITRDB

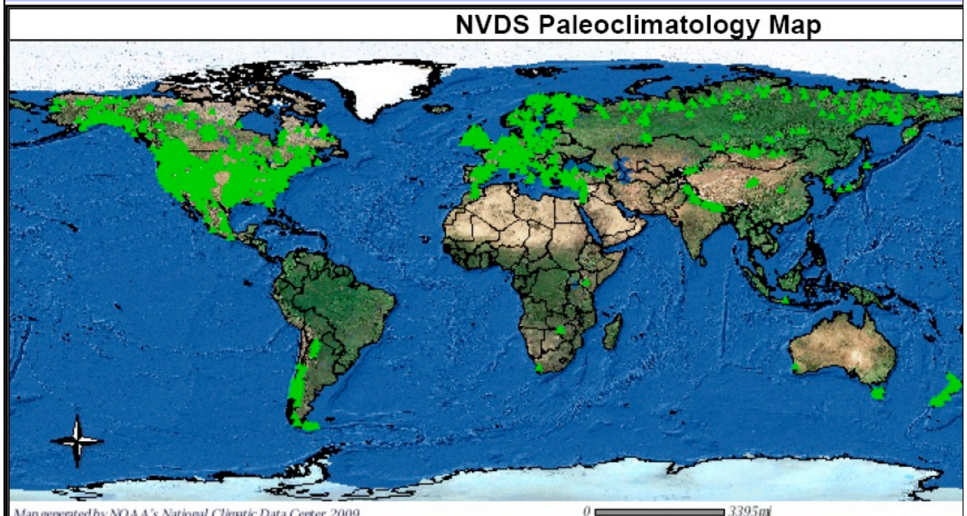

87 chronologies 1000+ years world-wide, of which 59 are in U.S.

http://www.ncdc.noaa.gov/paleo/treering.html

Tree-Ring Chronologies, >250 years in length

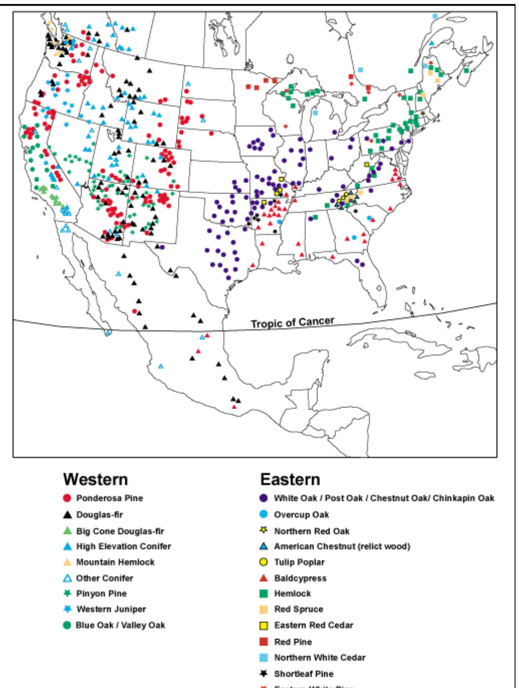

54 of the 59 1000+ years chronologies in U.S. are in the western U.S.

(D. Stahle, The Unsung Ancients. Natural History Magazine (Feb 2002)
http://www.naturalhistorymag.com/master.html?http://www.naturalhistorymag.com/0202/0202_feature.html

Carbon-13 Variations in Sequoia Rings and the Atmosphere

Harmon Craig[1]
Institute for Nuclear Studies, University of Chicago, Chicago, Illinois

RECENTLY THE WRITER presented data on the isotopic composition of carbon in some 80 specimens of modern and fossil plants and coal (1). Modern land plants displayed a range of composition amounting to some 0.7 percent of the ratio C^{13}/C^{12}; the average depletion in

A complete radial of one of the oldest sequoias was obtained through the courtesy of Professor Edmund Schulman of the Laboratory of Tree-Ring Research, University of Arizona. He very kindly dated the rings of the radial specimen from the original dating of the tree by A. E. Douglass. Successive rings were cut out

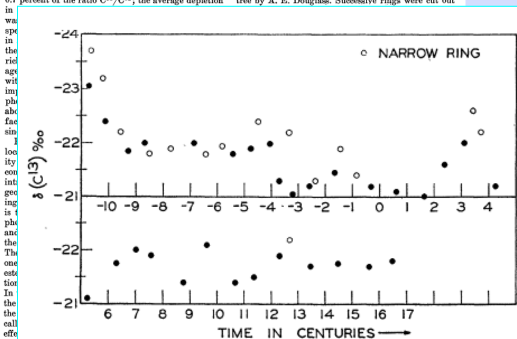

FIG. 1. Variation of carbon-13 concentration in annual rings of *Sequoia gigantea* from 1072 B.C. to A.D. 1649. Ordinal values represent C^{13} enrichment in per mil with respect to an arbitrary standard which has the isotopic composition of average marine limestone.

January 29, 1954 141

Early interest in the stable isotopes in tree rings

Science 119: 141-143 (1954)

It is clear that many more trees and more closely spaced rings from individual trees must be analyzed before any definite conclusions concerning the fine structure of such variations can be reached. The data indicate, however, that the isotopic composition of the atmospheric carbon was constant to at least 1 per mil during the 2500-year interval from 900 B.C. to A.D. 1600 with a change in mean composition probably less than 0.2 per mil. The considerations discussed above indicate that even the 1 per mil irregular variations in *Sequoia* are more probably due to the effects of varying external conditions on the assimilation and respiratory processes of the tree rather than to atmospheric changes. Future work on the cause of such variations should be worthwhile; nevertheless it should be stressed that such variations, while real enough, are of extremely small magnitude compared to the 4.5 percent variation encountered in nature. It is this aspect which is of considerable interest with respect to the application of what may be called "natural" isotopic tracer and dilution techniques to geochemical problems, and which will be discussed in this respect elsewhere.

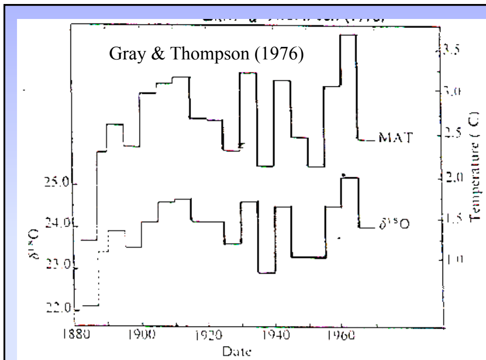

Fig. 2 A comparison between the mean annual temperature (MAT) curve obtained from the meteorological data and that obtained from $^{18}O/^{16}O$ ratios of cellulose. (The broken part of the isotope curve is calculated for some out-of-sequence rings that were not analysed.)

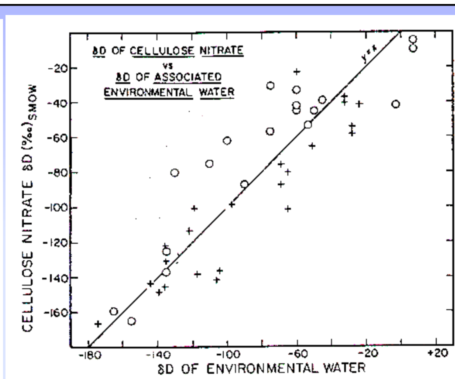

FIG. 2. A plot of the δD value of the nitrated cellulose from a variety of plants from a wide geographic range against the δD value of the associated environmental water. The open circles depict points for which the δD value of the environmental water was obtained from the literature

- Schiegl (1974) was the 1st to observe that δD of plant matter related to climate. Gray & Thompson (1976) argued that $\delta^{18}O$ in tree rings may act as a paleo-thermometer
- A 1:1 correlation exists between δD cellulose and δD of environmental water. (Yapp & Epstein, 1982)

Living trees

Destructive sampling (cross-sections)

Non-destructive sampling (cores)

Historical wood

<u>Buildings</u>: churches, castles, houses, barns.

<u>Other</u>: bridges, fences, walkways, tombs, frames.

Archaeological wood

(1) primary and secondary roof support beams
(2) window and door timbers
(3) hearths and firepits (often charcoalized)

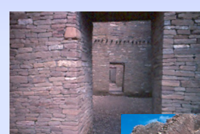

Wood from biological and geological deposits

alluvial deposits
lake deposits
bog deposits
packrat midden macrofossils
glacial deposits

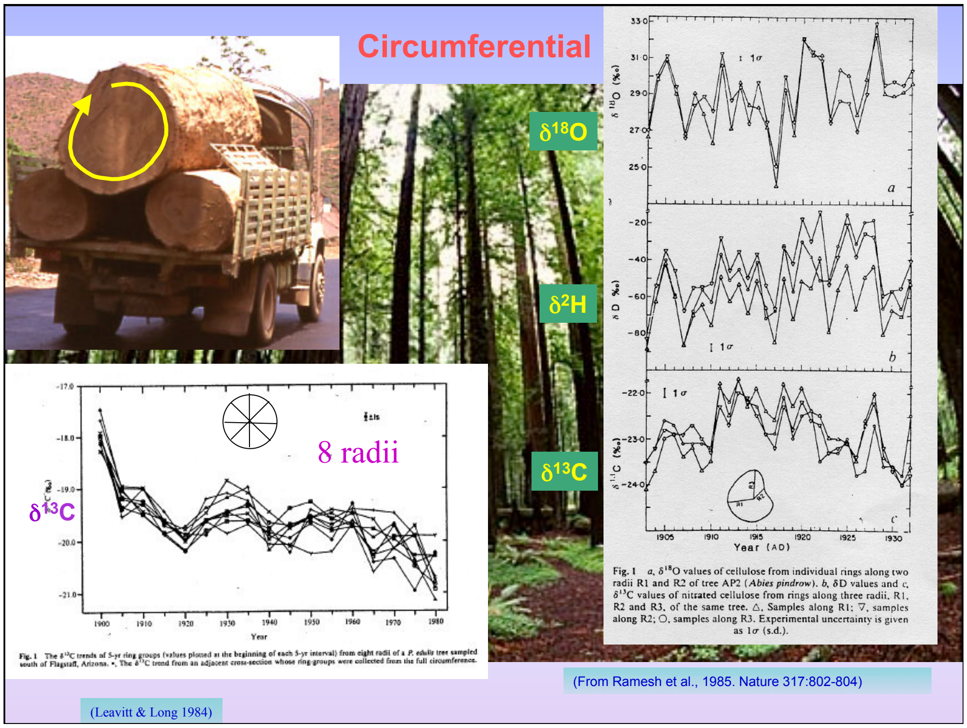
Circumferential
δ18O
δ2H
δ13C
8 radii
δ13C
Year (AD)
Fig. 1 a, δ18O values of cellulose from individual rings along two radii R1 and R2 of tree AP2 (Abies pindrow). b, δD values and c, δ13C values of nitrated cellulose from rings along three radii, R1, R2 and R3, of the same tree. △, Samples along R1; ▽, samples along R2; ○, samples along R3. Experimental uncertainty is given as 1σ (s.d.).
Fig. 1 The δ13C trends of 5-yr ring groups (values plotted at the beginning of each 5-yr interval) from eight radii of a P. edulis tree sampled south of Flagstaff, Arizona. •, The δ13C trend from an adjacent cross-section whose ring-groups were collected from the full circumference.
(From Ramesh et al., 1985. Nature 317:802-804)
(Leavitt & Long 1984)

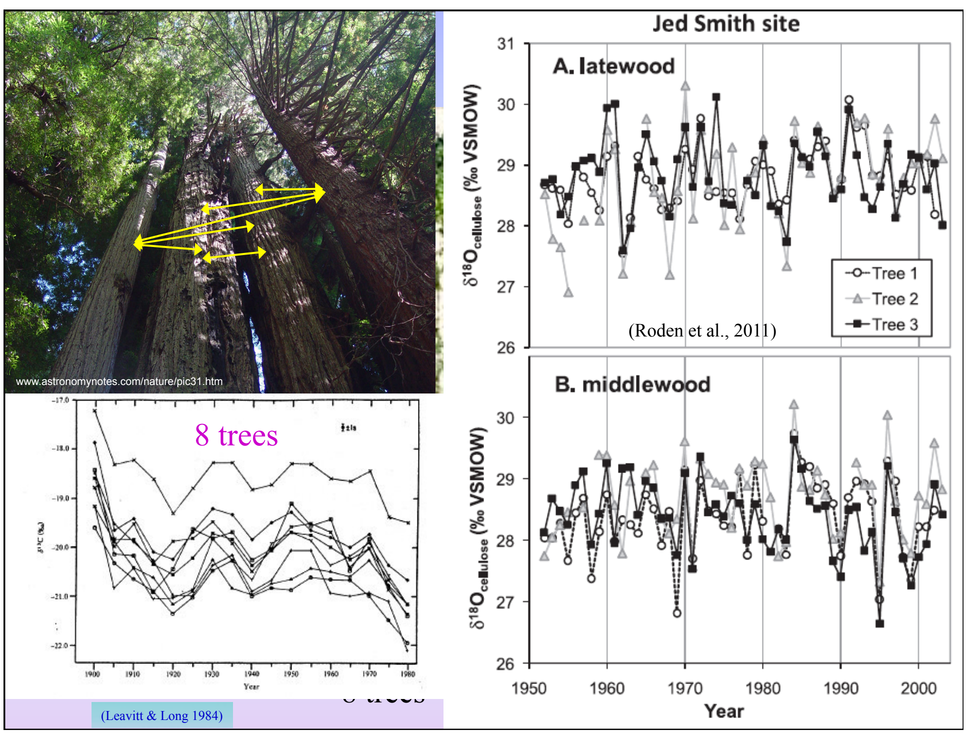
Jed Smith site
A. latewood
B. middlewood
δ18Ocellulose (‰ VSMOW)
Tree 1
Tree 2
Tree 3
(Roden et al., 2011)
Year
www.astronomynotes.com/nature/pic31.htm
8 trees
(Leavitt & Long 1984)

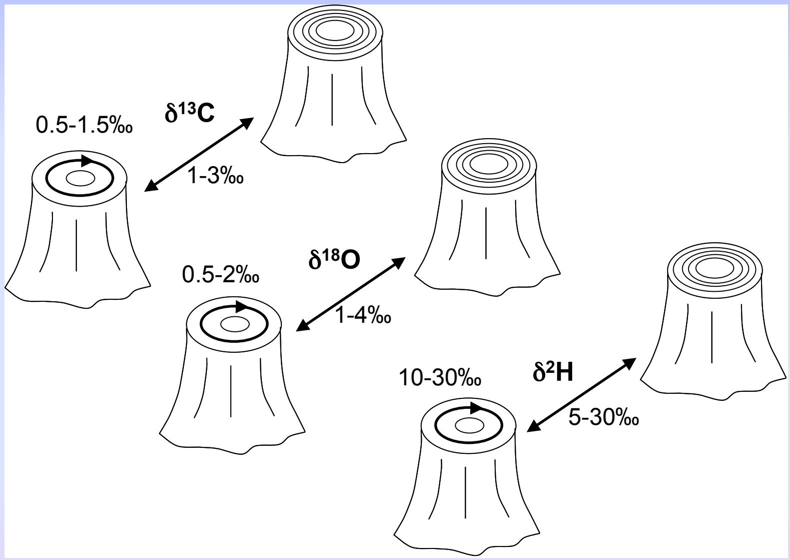

See Leavitt (2010) for a review of isotope variability and sampling strategies.

Cellulose purification may be necessary since different components of wood are isotopically distinct.

• Leavitt and Danzer (1993) modified the “Jayme-Wise” technique for batch processing small wood samples

• The steps involve
1. Soxhlet extraction using toluene:ethanol (2:1) then pure ethanol to remove lipids waxes and oils.
2. Boiling with DI water to remove salts and low MW polysaccharides
3. A sodium chlorite - acetic acid solution “bleaching” to remove lignin
4. Strong NaOH to remove hemicellulose
5. Acetic acid and DI rinse → α-cellulose

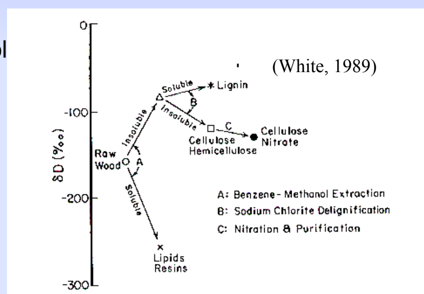

Figure 10.5. The δD values of several fractions of organic compounds. The organic fractions are arranged from left to right in the order of chemical treatments commonly used in analyzing wood from trees, beginning with raw wood and ending with cellulose nitrate. The data are primarily from Epstein et al. (1976).

• QA standards might also be included in the cellulose extraction (Porter and Middlestead (2012)

• Modifications of this method can be found in Loader et al. (1997), MacFarlane et al. (1999) and Brendel et al. (2000). A number of recent papers have also compared the various methods utilized to obtain cellulose (Cullen and Macfarlane, 2005; Gaudinski et al., 2005: Rinne et al., 2005; Harlow et al., 2006, Gori et al., 2012, Kagawa et al., 2015, Fines-Neuschild et al., 2015, Lin et al., 2016).

Comparisons with whole wood indicate that cellulose may not be required for climate reconstruction using δ^{18}O.

• Whole wood, α-cellulose and lignin have been positively correlated with modeled source water δ^{18}O, temperature and humidity (Barbour et al. 2001). A The whole wood/cellulose relationship has a slope of 1 for δ^{13}C but not for δ^{18}O. →

Roden and Farquhar (2012)

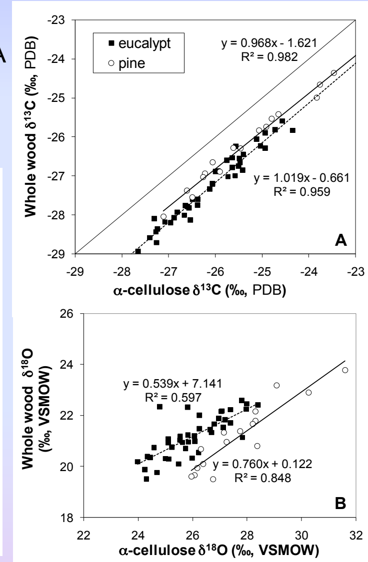

• There are significant differences between whole wood and α-cellulose and some climate information may indeed be lost. However, this could be offset by greater sample throughput and replication (Borella et al. 1999, Weigt et al., 2015).

Borella et al. (1999)

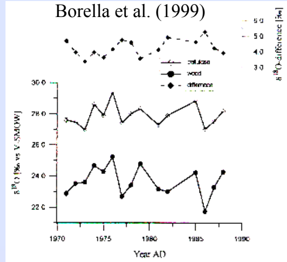

Figure 3. The δ^{18}O of cellulose and toluene-ethanol extracted wood (open diamonds and solid circles, respectively), from an oak of the Swiss "Mittelland," and differences between them (solid diamonds). The differences are not correlated with the δ^{18}O values either of wood or of cellulose. (This study is mainly restricted to the time period 1971 to 1994 due to the availability of δ^{18}O from precipitation for this period. A more detailed climatic interpretation of the tree ring δ^{18}O data used in this paper will be the subject of another paper still in preparation.)

However, for a different view see Battipaglia et al., (2008).

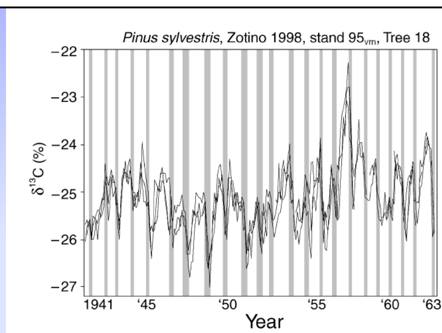

Figure 8. Radial course of δ^{13}C in a core of Scots pine Tree 18 between the years 1941 and 1963. Lines represent three adjacent parallel traces of laser ablation holes that were shot moving back and forth in blocks according to the scheme in Figure 2. Vertical gray bars indicate the latewood area of individual tree rings.

Laser ablation and micro-milling techniques

(Schulze et al. 2004)

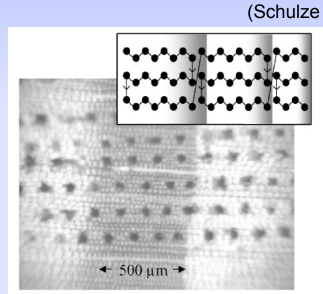

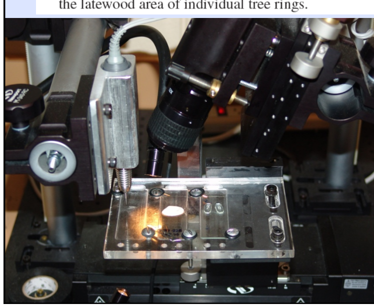

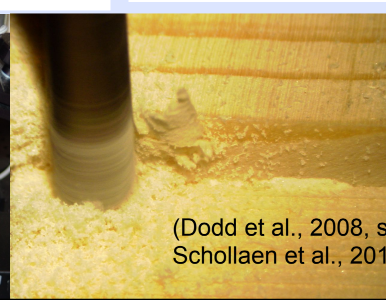

Computer-controlled micromilling

(Dodd et al., 2008, see also Schollaen et al., 2014)

The ultimate source of ^{13}C in organic matter is atmospheric CO_2 through the process of photosynthesis. That source, however, has not been stable over time and must be accounted for in tree ring $\delta^{13}C$ studies.

Ice core records provide data for atmospheric CO_2 concentration and $\delta^{13}C$ variation that extend beyond 20th century measurements.

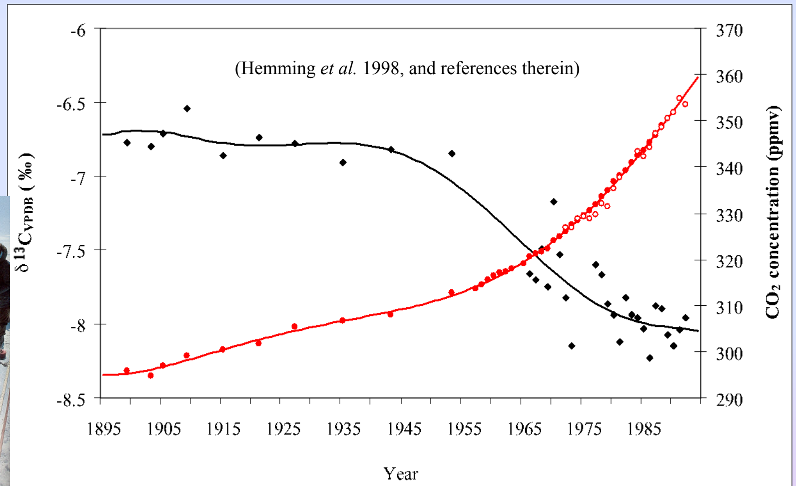

Isotopic composition of different wood compounds

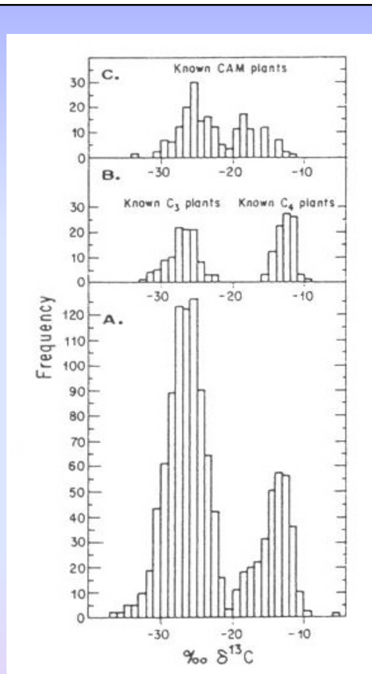

← $\delta^{13}C$-values of photosynthetically fixed carbon
A. Terrestrial plants, B. C_3 and C_4 plants, C. CAM plants

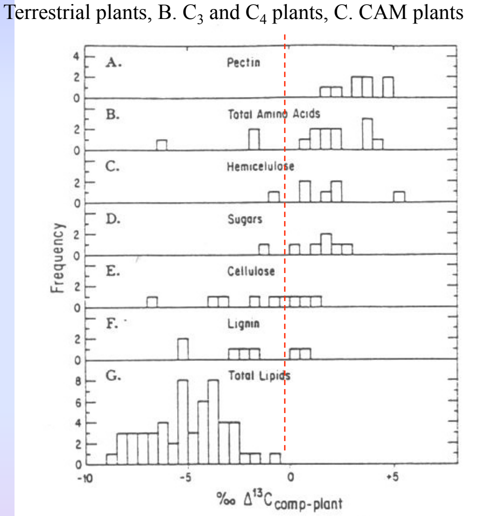

$\Delta^{13}C$-values of plant constituents

(Deines, P. In: Fritz & Fontes. 1980. Handbook of Environmental Isotope Geochemistry V.1. The Terrestrial Environment. Elsevier.)

Sources of hydrogen in cellulose

- All the H in organic matter comes from water (recall Todd's lecture on variation in meteoric waters). Most from water taken up by roots, but some also from atmospheric vapor.

- Photosynthetic electron transport discriminates against D forming a pool of reductant (NADPH) enriched in H. δD can be depleted by as much as -120 to -171‰ (Estep and Hoering, 1981, Yakir and DeNiro 1990)

- An additional fractionation can occur during the biosynthesis of proteins and lipids during gycolysis (as much as -30 to -60‰) (Estep and Hoering, 1981)

- Post-photosynthetic carbohydrate metabolism causes an enrichment in D in carbon bound hydrogen atoms. (from 144 to 166‰) (Luo and Sternberg 1992, Yakir and DeNiro 1990)

Sources of oxygen

- Oxygen could come from either CO_2 or water, but when CO_2 goes into solution it quickly exchanges its O with the much more abundant water (DeNiro and Epstein, 1979).

- $\delta^{18}O$ in cellulose is 27 ± 3‰ enriched compared to source water. (Sternberg and DeNiro, 1983)

- Enrichment is associated with water/carbonyl interactions

$$R_2C=O + H_2O^* \leftrightarrow R_2C(OH)(O^*H) \leftrightarrow R_2C=O^* + H_2O$$

- The amount of exchange may be dependent on the amount of triose-P cycling. (Farquhar et al. 1998)
  Fructose 1,6-bisphosphate ↔ DHAP + G3P

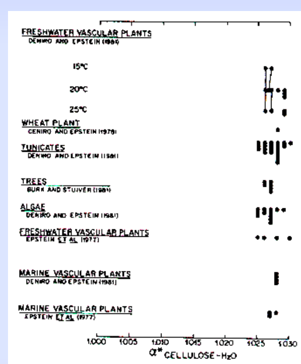

Fig 1. Sternberg and DeNiro, 1983

- The 27‰ enrichment is valid for most applications, but a number of studies have shown that reality (as always) can be more complicated (Schmidt et al. 2001, Sternberg et al. 2006, Sternberg and Ellsworth 2011)

$\delta^{13}C$ analysis of cellulose

Cellulose or whole wood is combusted on-line in a oxidizing column with catalysts and the gas products are separated (CO_2, N_2) or trapped (H_2O) for analysis.

$\delta^{2}H$ analysis of cellulose

• The H on all C-OH groups are exchangeable with medium water and are thus modified after being laid down (C-H hydrogen do not exchange). Therefore, these H **do not** reflect past environmental conditions.

• There are two methods for eliminating C-OH hydrogen.

1. The isotopic equilibrium technique attempts to exchange all the C-OH hydrogen using water of a known $\delta^{2}H$ and then back calculate the original non-exchangeable values. (Friedman et al. 1988; Schimelman et al., 1993, Wassenaar and Hobson 2000)
2. The exchangeable H are removed and replaced with nitrate (nitration) using strong nitric acid and acetic anhydride then purified by dissolving in acetone.

• Cellulose nitrate is combusted in the presence of cupric oxide and a Zn catalyst converting it to H_2 gas for analysis.

$\delta^{18}O$ analysis of cellulose

• The most common method is an on-line pyrolysis that converts organic matter to CO at high temperatures using a column in an elemental analyzer and a glassy carbon column. (Farquhar et al., 1997; Saurer et al. 1998)

• The on-line method may have memory effects, but the rapidity of throughput and replication offsets any disadvantages.

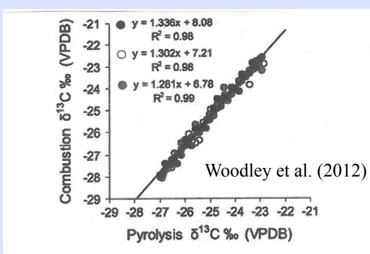

Figure 2. The adjustment procedure requires accurate determination of the slope between pyrolysis and combustion datasets. This is achieved by sampling the range of the pyrolysis dataset at 30 equidistant intervals and then re-analysing these samples using combustion. Three independent samples ($n = 30$) were taken from the pyrolysis chronology at Southern Glens using adjacent data points. The relationship between the two methods and between each of three datasets is very strong ($R^2 > 0.98$). The dashed line represents the slope of the 3074 individual combustion and pyrolysis measurements.

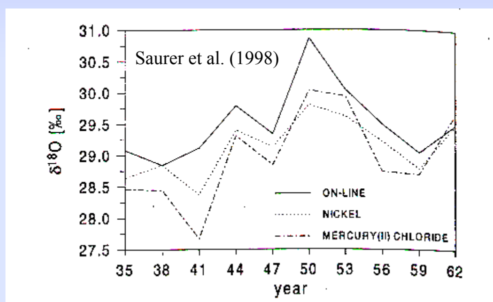

Figure 4. Tree ring sequence measured with (1) the on-line, (2) the mercury(II) chloride and (3) the nickel methods.

• Recent work is highlighting the possibility of obtaining both $\delta^{13}C$ and $\delta^{18}O$ data from the same sample. (Woodley et al., 2012, Loader et al., 2015)

C Fractionation in C_3 Plants (recall from Jim's lecture)

$$\delta^{13}C_{C3\ plant}\ (‰) = \delta^{13}C_{air} - a - (b - a) \times c_i/c_a$$

a is the fractionation by diffusion into the stomata (4.4‰)
b is the fractionation caused by RuBP carboxylation (reported as *ca.* 27-30‰),
$\boldsymbol{c_i}$ is the concentration of CO_2 in the intercellular leaf space,
$\boldsymbol{c_a}$ is concentration of CO_2 in air

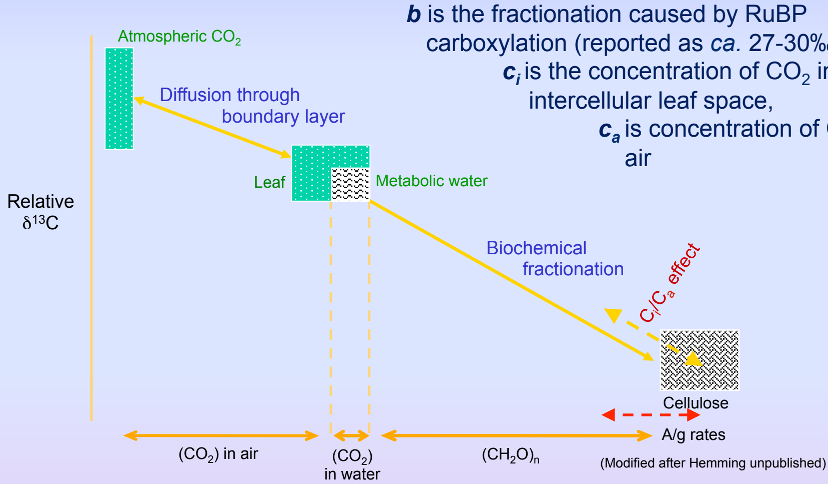

Schematic of relative $\delta^{13}C$ fractionations involved in cellulose synthesis

Models requirements for the isotopes of water can be visualized

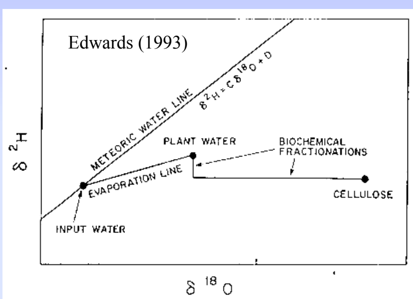

Fig. 1. Graphical representation of the Edwards and Fritz [1986] model. Potential paleoclimate signals exist in displacement along the meteoric water line (which may provide proxy temperature) and along the evaporation line (inverse to photosynthetic humidity). Note that the sensitivity of the model varies depending on the sense of climatic variation in meteoric water $\delta^{18}O$ versus h space, as the meteoric water and evaporation lines are not orthogonal.

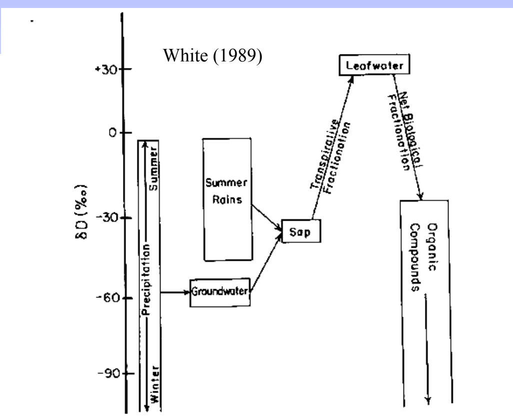

Figure 10.1. A generalized picture of the changes in the stable hydrogen isotope ratios in the hydrogen pathway in plants. The δD values are typical for plants growing in the northeastern United States.

The main inputs are source water, some estimate of leaf water enrichment and biochemical fractionation.

We start with leaf water

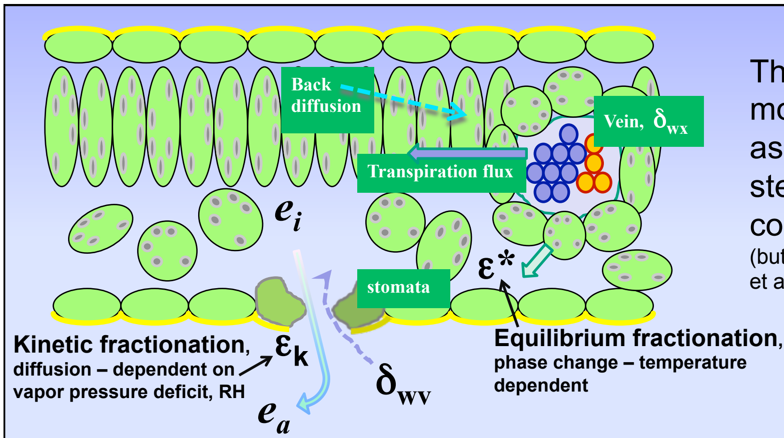

These models assume steady-state conditions (but see Cernusak et al. 2002, 2005).

Craig and Gordon (1965) were the first to model the effects of evaporation on bodies of water. Dongman et al. (1974) formulated a leaf water model (recall Todd's lecture).

$$\delta_{wl} = \delta_{wx} + \varepsilon_k + \varepsilon^* + (\delta_{wv} - \delta_{wx} - \varepsilon_k) \bullet e_a / e_i$$

e is vapor pressure and the subscripts: ***wl*** = leaf water, ***wx*** = xylem water, ***wv*** = water vapor, ***i*** = intercellular, ***a*** = atmospheric (ambient)

• Roden et al. (2000) proposed a modification of the previous mechanistic models to account for the variation in the isotopic composition tree ring cellulose.

$$\delta D_{cellulose} = f_H \bullet (\delta D_{ws} + \varepsilon_{HH}) + (1 - f_H) \bullet (\delta D_{WL} + \varepsilon_{HA})$$
$$\delta^{18}O_{cellulose} = f_O \bullet (\delta^{18}O_{ws} + \varepsilon_O) + (1 - f_O) \bullet (\delta^{18}O_{WL} + \varepsilon_O)$$

• Leaf water (δ_{WL}) is estimated from the modified Craig-Gordon evaporative This parameter contains the environmental information regarding humidity, atmospheric vapor δD and $\delta^{18}O$ etc.

• ***f*** is the proportion of carbon bound H or O that undergoes exchange with medium water.

• ε_{HH} is a heterotrophic fractionation factor during cellulose synthesis (≈ +158‰) Yakir& DeNiro 1990

• ε_{HA} is an autotrophic fractionation factor during photosynthetic carbon fixation (≈ -171 ‰) Yakir& DeNiro (1990), Luo & Sternberg (1992)

• ε_O is ~ 27‰ from the water carbonyl interaction and does not differ between heterotrophic and autotrophic metabolism.

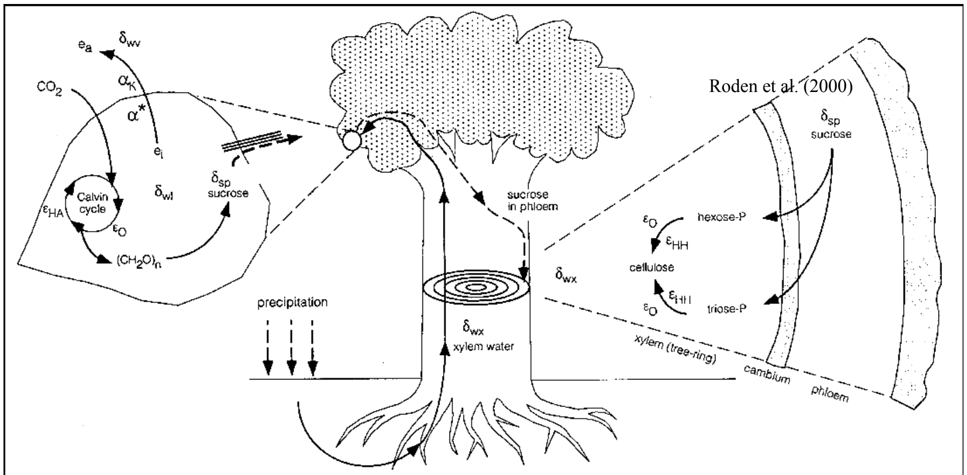

Fig. 1. A diagram of the isotopic fractionation events occurring between precipitation input and tree-ring cellulose.

• This model has been demonstrated to work for field grown plants as well. (Roden & Ehleringer, 2000)

• The model assumes all carbon comes from current photosynthate (not from stored reserves, which Terwilliger asserts are important) and this may be problematic for earlywood studies. See also Offermann et al., 2011 for uncoupling of cellulose $\delta^{18}O$ from leaf signals.

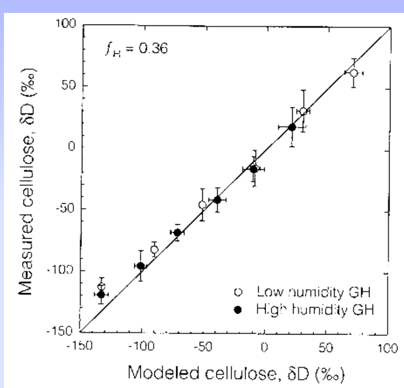

Fig. 7 The relationship between the δD of modeled and measured tree-ring cellulose. Variations in tree-ring cellulose were generated by altering source water δD in a hydroponic system in a controlled greenhouse environment at either high or low relative humidity. *Values* are means and SDs. The *line* represents a 1:1 relationship

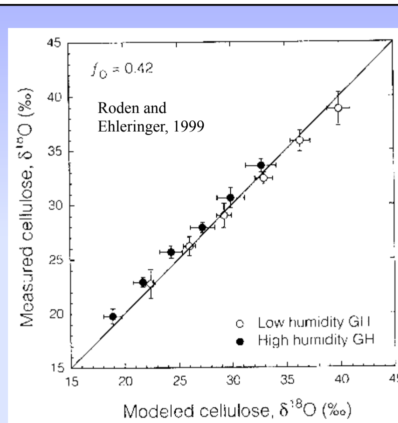

Fig. 8 The relationship between the $\delta^{18}O$ of modeled and measured tree-ring cellulose. Variations in tree-ring cellulose were generated by altering source water $\delta^{18}O$ in a hydroponic system in a controlled greenhouse environment at either high or low relative humidity. *Values* are means and SDs. The *line* represents a 1:1 relationshi

• Using this model Roden & Ehleringer (1999) predicted the cellulose δD and $\delta^{18}O$ values obtained from their controlled hydroponics experiment.
• The model predicted the tree ring isotopic composition including the variation due to differences in source water and humidity.
• The differences between ε_{HH} and ε_{HA} (+158 vs -171‰) offset each other making the cellulose vs. source water relationship appear to be 1:1.

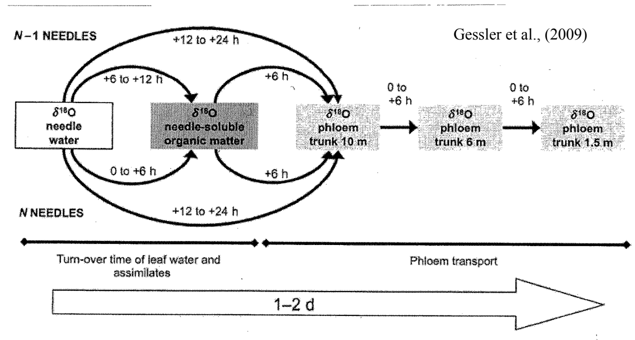

Figure 4. Tracing the oxygen isotope signal through the tree. Significant time-lagged correlations between $\delta^{18}O$ in different tree compartments (cf. Fig. 2d): needle water and water-soluble organic matter for current year (*N*) and previous year (*N* − 1) needles, phloem sap in the trunk bark at three sampling heights (10, 6 and 1.5 m height). The figure is adapted from Barnard *et al.* (2007).

A number of studies are attempting to incorporate assimilate transfer, carbohydrate pools, exchange and downstream metabolic processes into these mechanistic models to further clarify sub-annual $\delta^{18}O$ variation in tree ring cellulose.

For pine, $\delta^{18}O$ signals from the leaf were transferred to the tree-ring with a 2 week time lag. (Gessler et al., 2009)

For beech, the reliance on stored carbohydrates led to an uncoupling of leaf and tree-ring $\delta^{18}O$. (Offermann et al., 2011). Differences in phloem loading and corticular C gain may lead to variation in f_O (> 0.42) (Gessler et al. 2013)

(see also papers by Kagawa et al., 2005, 2006, Keel et al., 2007; Gessler et al., 2014, Barbour and Song, 2014, Kimak et al. 2015)

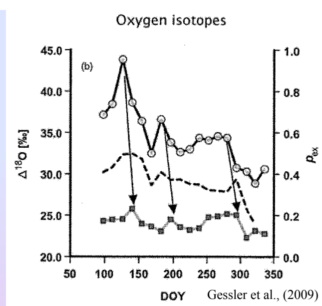

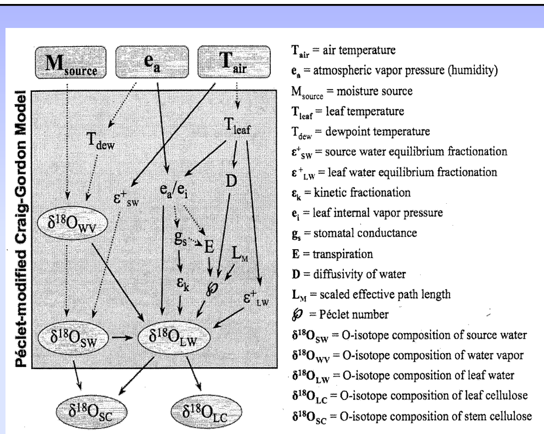

Fig. 1. Schematic illustration showing the functional relationships between the primary model variables (rounded squares) and secondary model variables (symbols within the shaded box) that influence leaf cellulose $\delta^{18}O$ and stem cellulose $\delta^{18}O$ in the Péclet-modified Craig–Gordon (PMCG) model. All variables containing isotope values (secondary variables as well as model outputs) are highlighted in ovals. Solid lines represent functions contained in the original PMCG model,

Khamen et al. (2011) further tested these models to determine the influence of humidity (e_a) and air temperature (T_{air}) in tropical ecosystems.

They found e_a and T_{air} both influence ^{18}O enrichment and that they may both integrate into a single index: the leaf to air vapor pressure deficit (VPD)

A robust relationship between VPD and $\delta^{18}O$ in cellulose was observed.

Reducing the number of parameters required to describe O isotope variation is desirable for paleo-reconstructions.

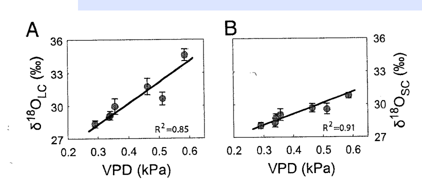

Fig. 4. The relationship between mean annual leaf-to-air vapor pressure difference (VPD) and $\delta^{18}O$ values in (*A*) leaf and (*B*) stem cellulose for measured values across the seven sites along the Mauna Loa gradient. Error bars represent 1 SD, *n* = 5.

Modeling isotope variation in tree rings presents a dichotomy.

Researchers have made great strides in revealing the complexity of H and O isotope fractionation and exchange processes. But advances in complexity make the utilization of those models for interpreting isotope variation in ancient tree rings problematic. They cannot be parameterized.

Others simplify isotope modeling by concentrating on a few key parameters hoping to capture the most important environmental variation. Many studies ignore modeling altogether and simply use statistical correlations with climate records to make inferences about past climates.

Lets review and simplify. Carbon isotope variation in organic matter can be divided into 3 main components.

1. **Source** of CO_2 and its $\delta^{13}C$ value.

2. **Supply** of CO_2 to the chloroplast (stomatal conductance).

3. **Demand** for CO_2 in photosynthesis (rates & capacity).

And depending of the substance studied.

4. Post-photosynthetic fractionation (cellulose, OK 1^{o})
5. Retrieval from storage

Do the following data sets then make sense?

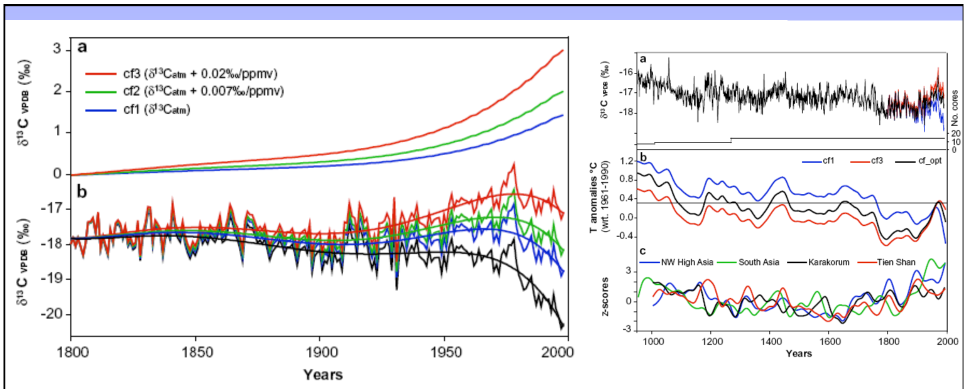

Fig. 2. (a) Correction factors since 1800 (cf) for changes in the atmospheric $\delta^{13}C$ (cf1), and accounting for plant physiological responses on atmospheric pCO_2 changes by increased discrimination after Kürschner (1996) (cf2) and Feng and Epstein (1995) (cf3). (b) Corrections applied to the tree-ring $\delta^{13}C$ record 'Mor'.

Corrections for atmospheric $\delta^{13}C$ and pCO_2

Declines in tree ring $\delta^{13}C$ in the 20[th] century are not related directly to climate but to burning of fossil fuels. Corrections may need to be both isotopic and physiological.

(Tryedte et al., 2009)

Standardized cellulose $\delta^{13}C$ of *Fagus sylvatica* tree rings from two dry sites 50 km apart compared to precipitation.

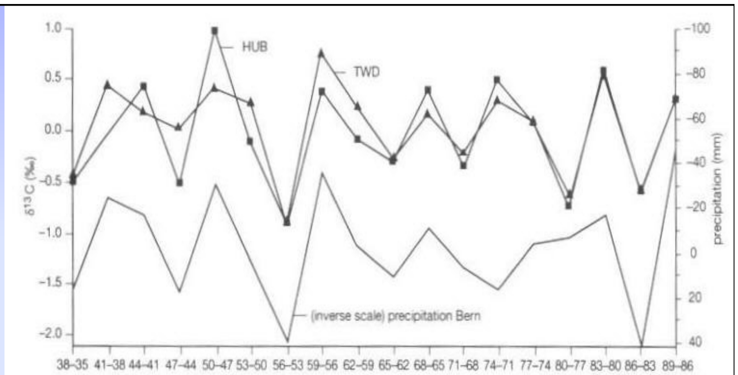

(Saurer et al. 1995)

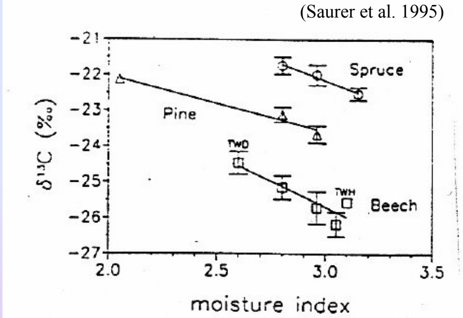

$\delta^{13}C$ and Precipitation Amount

Tree ring $\delta^{13}C$ for three European species related to measures of water availability.

δ^{13}C and VPD

Reconstruction of atmospheric vapor pressure deficit using δ^{13}C of ***Pinus sylvestris*** tree rings in England

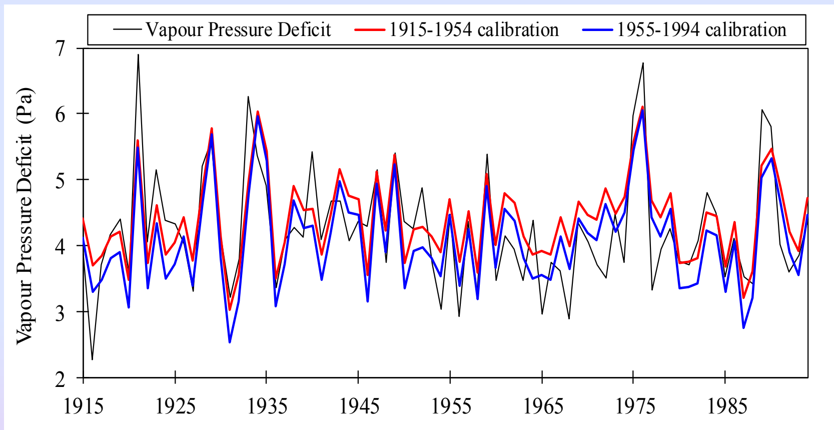

(Hemming et al. 1998)

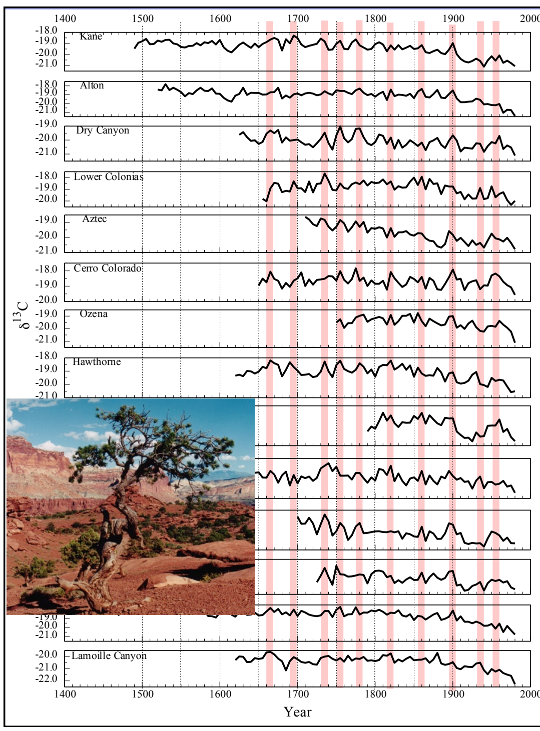

δ^{13}C & Water Use Efficiency

Southwest Pinyon pine isotope Network (Leavitt & Long 1988,1989)

Long-term declining trends (increasing iWUE?) and short-term fluctuations common across hundreds of kilometers in some instances (see also Saurer et al. 2014)

From Eddy Flux data

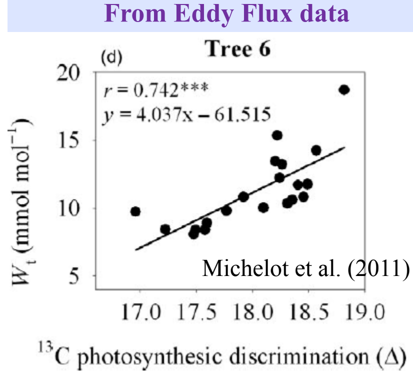

Modified from Roden and Farquhar (2012)

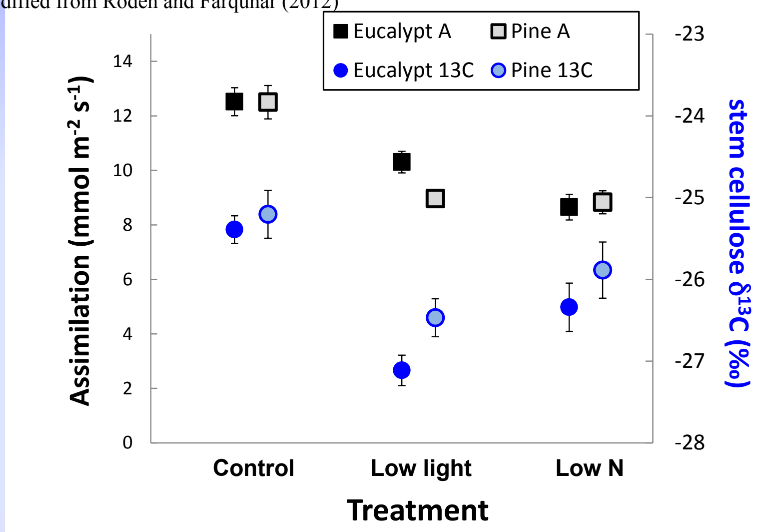

The demand side (photosynthesis) can affect tree ring cellulose. Some extract temperature information from $\delta^{13}C$ (Esper et al. 2015).

Review and simplify! Oxygen and hydrogen isotope variation in organic matter can be divided into 3 main components.

1. **Source of H_2O** for leaves and its $\delta^{18}O$ or $\delta^{2}H$ value
2. **Atmospheric vapor** $\delta^{18}O$ or $\delta^{2}H$ (related to source?)
3. **Evaporative enrichment** of leaf water (driven by VPD)
4. Biochemical fractionation (constant or dependent?)
5. Proportional exchange with water at site of synthesis (constant or variable? See Song et al., 2014)

And depending of the substance studied.

6. Post-photosynthetic fractionation (cellulose – OK)
7. Retrieval from storage

Do the following data sets then make sense?

Variability associated with humidity

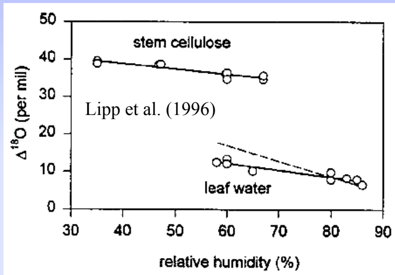

FIG. 3. Relative humidity vs. normalized leaf water and stem cellulose oxygen isotope composition of *Tamarix jordanis*. The dashed line represents the expected Craig evaporative-enrichment response of leaf water (e.g., see Buhay et al., 1996). See text for discussion (data from Tables 1 and 2).

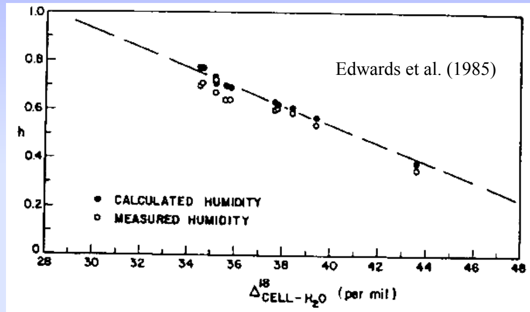

FIG. 2. Total measured cellulose–source-water isotopic difference versus measured and calculated humidity. The dashed line represents humidity calculated using fixed average values for ϵ_c and $\Delta^{18}_{CELL-LW}$, as explained in the text.

- $\delta^{18}O$ (and $\delta^{13}C$) of stem cellulose decreased with increasing RH - may be related to variations observed in leaf water. (Lipp et al. 1996)
- Combination of $\delta^{18}O$ and $\delta^{13}C$ may allow separation of 1° signals (source water and RH).
- RH is a dominant influence on variation in cellulose $\delta^{18}O$. (Edwards et al. 1985)
- Difficult to get representative data for humidity - RH is highly variable.

Temperature change with climate

Epstein, 1995

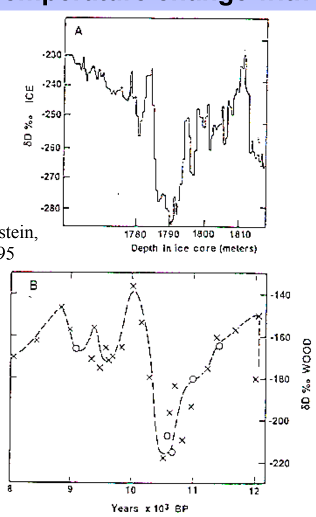

Figure 1. (a) The δD record of the ^{14}C-dated willow shrub samples from the north slope of Alaska, as compared to (a) an exact copy of an enlarged version of the published DYE 3 ice core data from Greenland [*Dansgaard et al.*, 1989]. The δD values of the ice cores are plotted against depth of the ice core samples on the ice cap. (b) The points marked with crosses have a suggested analytical uncertainty of ±160 years, whereas the open circles in Figure 1b have been determined by the AMS technique with an error of ±80 years.

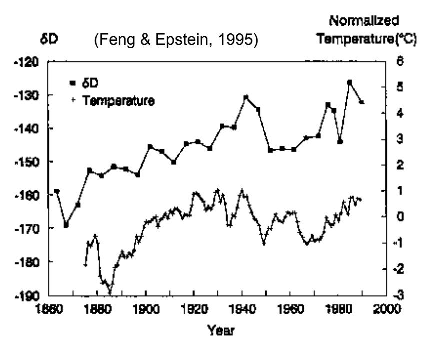

FIG. 8. Time series of the δD of WUOM-1 and the normalized temperature. The data points of the δD values are plotted at the middle year of the 5-year segment of wood, and the temperature is the 5-year running average of mean annual temperatures.

- Synchronous variations in δD records from ice cores and willow remains (^{14}C dated) are impressive and clearly show climate change during the Younger-Dryas events (Epstein, 1995).
- Correlation between δD and low frequency variation in temperature. (Feng & Epstein, 1995)

Variability associated with precipitation

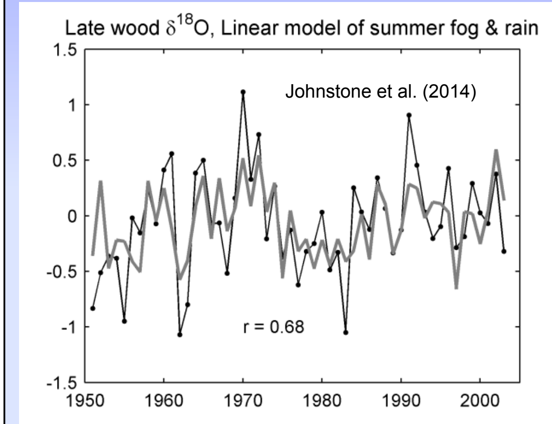

- A model that combines precipitation and fog variation is strongly correlated to latewood $\delta^{18}O$ variation. (Johnstone et al. 2014)

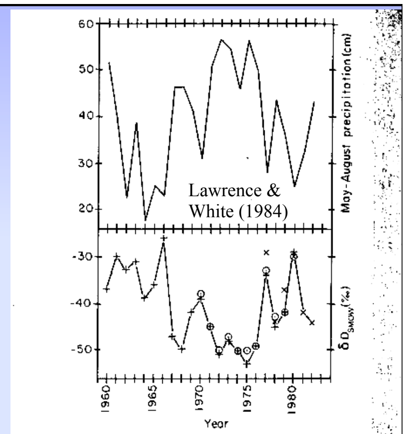

Fig. 1 Average amount of precipitation for the period May-August for five meteorological stations (Mohonk Lake, Poughkeepsie, Ellenville, Gardiner and Rosendale) plotted as a function of time. The δD values of rain and carbon-bound hydrogen from tree rings of two Eastern White Pine trees are also plotted. One tree covers the period 1960–80 (+), the other the period 1970–80 (O) and the rain from 1977–82 (×). The correlation coefficients between the δD values and the amount of May to August precipitation are −0.76, −0.93 and −0.88 respectively.

- Strong correlation between δD of cellulose and summer rain. (Lawrence & White, 1984 also Brienen et al, 2012, Williams et al., 2012 Rinne et al., 2013 on $\delta^{18}O$ precipitation proxies)
- Isotopic variation in precipitation from year to year at a single location have not yet been clearly related to mean temperature variation.

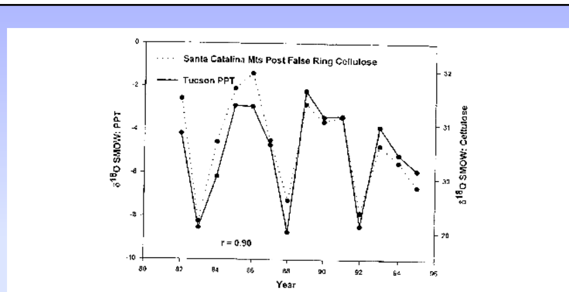

Figure 8 August-through-September weighted mean $\delta^{18}O$ in Tucson precipitation and $\delta^{18}O$ values from Santa Catalina Mountains cellulose after the false latewood band (summer wood)

- High correlation between false latewood band $\delta^{18}O$ and growing season precipitation $\delta^{18}O$ (the Arizona summer monsoon)

Wright et al. (1998)

- Correlated Tucson August-Sept precipitation and cellulose $\delta^{18}O$ with eastern Pacific sea surface temperatures.

- Best fit lag times were from between 11 to 15 months. Lag may be related to proximity of marine source, but uncertain.

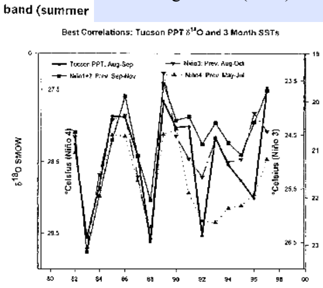

Figure 9 $\delta^{18}O$ values from Santa Catalina Mountains cellulose after the false latewood band plotted against three-month sea surface temperature means at the lags showing the highest correlations with August-through-September weighted mean $\delta^{18}O$ in Tucson precipitation

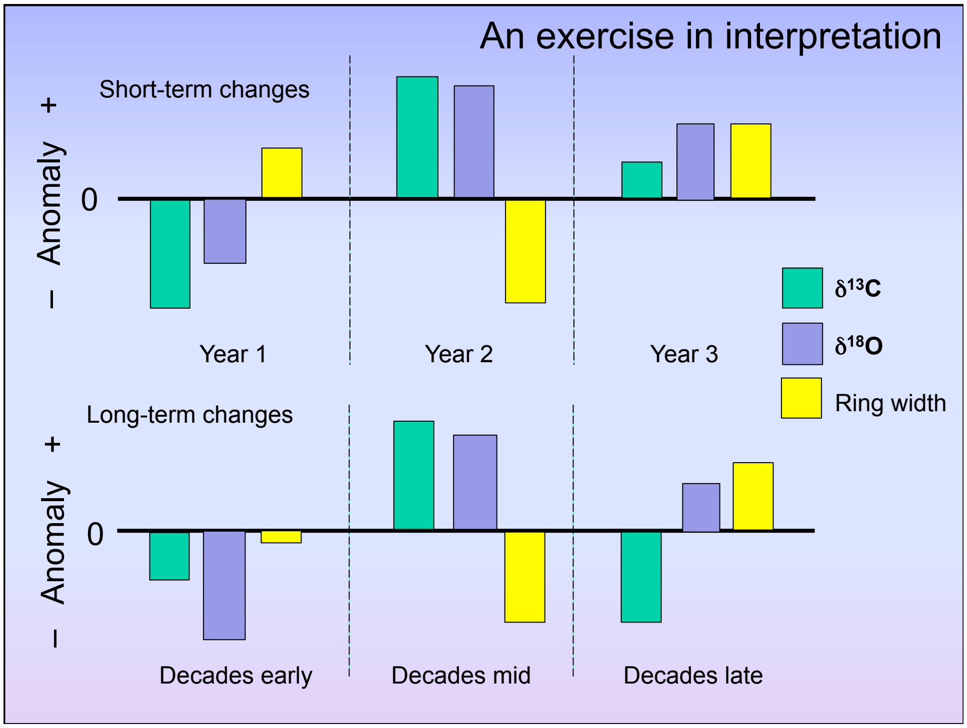

An exercise in interpretation
Short-term changes
+
Anomaly
0
–
Year 1
Year 2
Year 3
δ13C
δ18O
Ring width
Long-term changes
+
Anomaly
0
–
Decades early
Decades mid
Decades late

Where is the most appropriate location to sample the ring?
Earlywood?
Latewood?
Middlewood?
False latewood?
All of the above?

Seasonal variations of tree-ring $\delta^{13}C$ of a) ***Populus nigra***, b) ***Fagus sylvatica*** and c) ***Quercus petraea***.

(Helle & Schleser 2004)

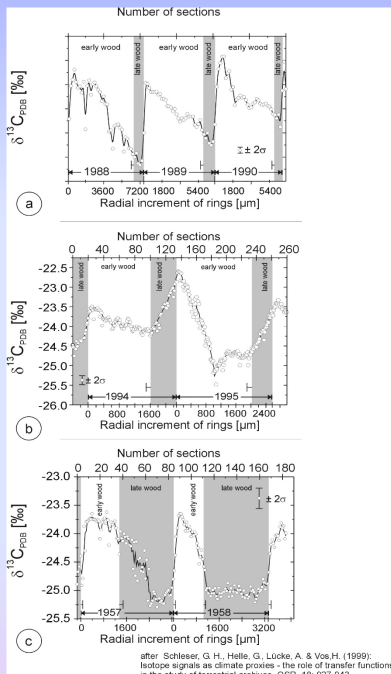

Seasonal variations of tree-ring $\delta^{13}C$ of ***Quercus petraea***, air temperature and precipitation Rostrevor, N-Ireland

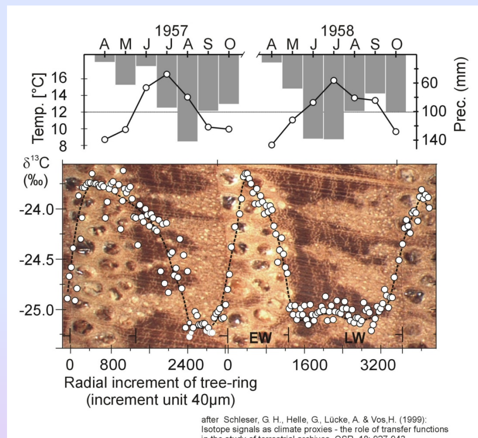

Intra-ring variability

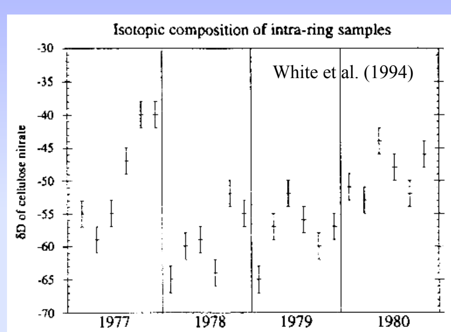

FIG. 2. Cellulose nitrate δD values for the intra-ring samples for the intermediate site white pine. Each of the four growth rings was divided into six sub-samples. The determination of the growth periods for the sub-samples is shown in Fig. 1.

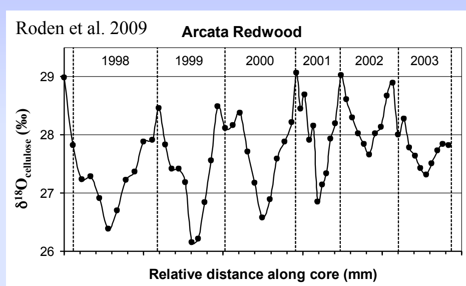

- Subdividing rings show variation in δD that might convey seasonal information - may be a biochemical thermometer. (White et al. 1994, Wilson & Grinstead, 1975)
- Variation in $\delta^{18}O$ in subdivided redwood helps to determine which portion of the ring is optimal for looking at seasonal variation in fog water inputs (Roden et al. 2009).
- Loader et al. (1995) subdivided rings with very high resolution (20 sample per ring) and intra-ring variability was associated with temperature and RH (see also Leavitt & Long 1991; Poussart et al. 2003, Berkelhammer and Stott, 2009, Kagawa et al., 2005, 2006; Keel et al, 2007; Gessler et al., 2009; Dodd et al. 2008, Managave et al., 2010 Schubert and Jaren 2011, Li et al., 2011, Schollaen et al., 2014).

The dual isotope approach

Some have argued that using both δ^{13}C and δ^{18}O may better constrain interpretation of δ^{13}C variation (Scheidegger et al. 2000, Grams et al., 2007).

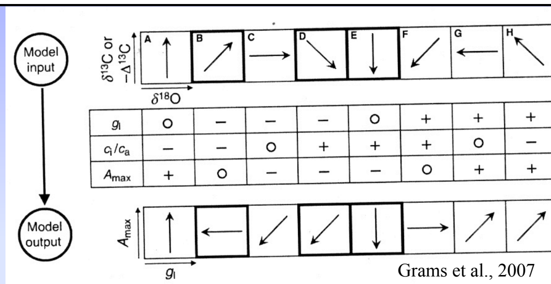

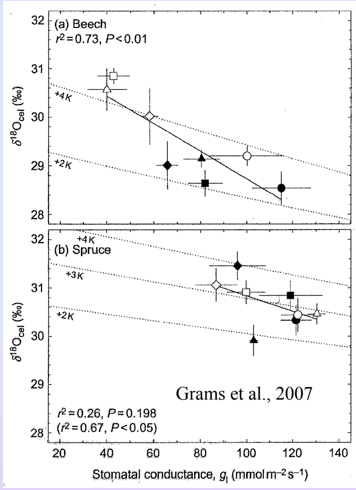

These conceptual models assume that δ^{18}O variation in organic matter is driven by variation is evaporative conditions (not source water changes) which will affect conductance to water vapor and thus internal [CO_2].

But be careful, there are many assumptions in these models that may not apply in every situation (see Roden and Farquhar, 2012; Roden and Siegwolf , 2012).

Strong relationships between stomatal conductance and cellulose δ^{18}O are not always found.

Cellulose models works for non-woody tissues like grasses.

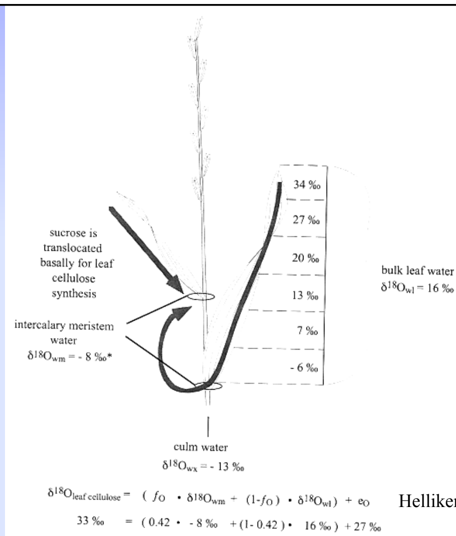

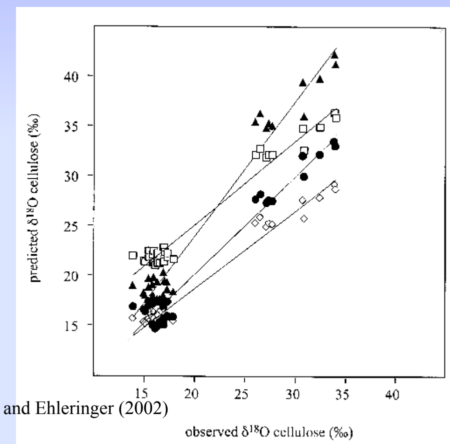

- Models need good estimates of leaf water for estimating δ^{18}O of sucrose exported.
- They also require an estimate of water δ^{18}O at the site of cellulose synthesis.
- Both estimates can be complicated by leaf anatomy and location of meristems.

Labelling can trace metabolic pathways

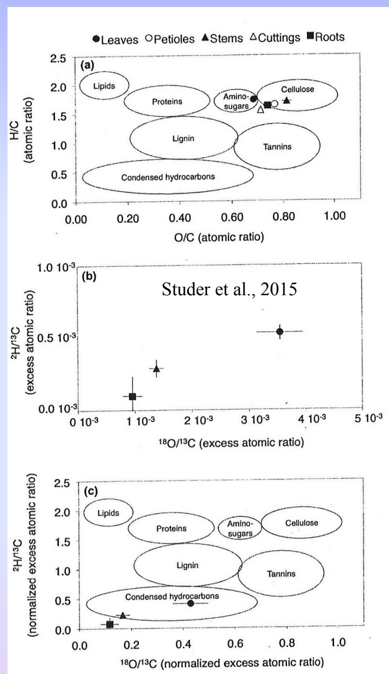

Multi-isotope (C, H & O through gas absorption) labelling of organic matter shows considerable back diffusion of vapor into leaves (>50% of leaf water signal) and that labelling can trace the incorporation of major elements of plant OM (and potentially soil OM). Studer et al. 2015

Figure 3. Atomic and isotopic ratios to illustrate change in OM characteristics. **(a)** Atomic and **(b, c)** isotopic ratios of oxygen and hydrogen to carbon within the leaves (black circles), petioles (white circles), stems (black triangles), stem cutting (white triangles) and roots (black squares). The circles overlain on the plots in **(a)** and **(c)** indicate atomic ratios characteristic for different compound classes (adapted from Sleighter and Hatcher, 2007). Panel **(a)** illustrates the atomic ratio of all tissues measured (15 replicates ± 1 standard deviation, panel **(b)** the isotopic ratios of the ^{13}C, ^{18}O and ^{2}H excess atom fraction (relative to the unlabelled tissues) measured after equilibrium in the labelling (see Fig. 1 and 2) was reached ($t = 8$ and 14, six replicates ± 1 standard deviation) and panel **(c)** shows the isotopic ratios after normalization with the maximum label strength detected in the leaf water (^{18}O, ^{2}H) and water-soluble OM (^{13}C).

Paleoclimate reconstruction

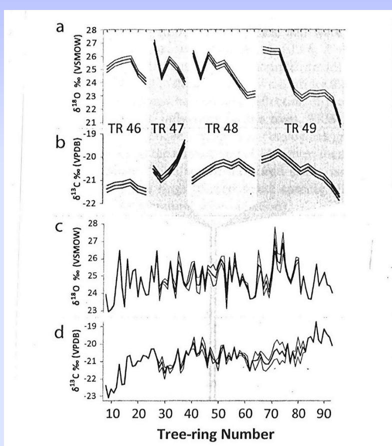

Figure 1. Subannual and annual-resolution time series records of tree-ring cellulose $\delta^{18}O$ and $\delta^{13}C$. Subannual resolution **(a)** $\delta^{18}O$ record, and **(b)** $\delta^{13}C$ record, of four tree rings (TR 46–49). Lines above and below the measured values (bold center lines) show the analytical uncertainty (0.14 ‰ for $\delta^{13}C$, 0.23 ‰ for $\delta^{18}O$). Annual resolution **(c)** $\delta^{18}O$ record, and **(d)** $\delta^{13}C$ record ($n = 86$). Bold lines show mean isotope values of annual-resolution study, thin lines above and below mean values show minimum and maximum isotope values of successfully crossdated tree-ring transects (TR 28–63, 64–82). Hook et al., 2015

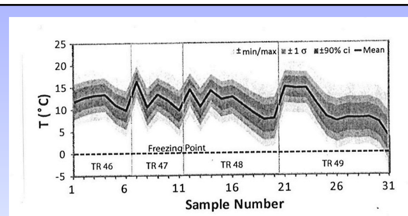

Figure 4. Mean temperature (°C) of subannual data based on all $\delta^{18}O$-temperature reconstructions. Mean of all reconstructions (black line) is bracketed by 90% confidence interval (±90% ci, dark gray fill), one standard deviation (±1 σ, medium gray fill), and minimum/maximum (± min/max, light gray fill). Freezing point is shown by dashed line.

Well-preserved wood from the Arctic Circle dated to the Eocene provides estimates of temperature using a reverse $\delta^{18}O$ cellulose model (Hook et al., 2015).

Temperature variation in the polar rainforest (even seasonal estimates) were on the order of 16 °C warmer than present.

In addition, estimates were made of plant water use efficiency (2x present) and multi-decadal climate cycles (PDO).

Obtaining direct source water $\delta^{18}O$ and δ^2H signals in cellulose may be possible.

The δ^2H variation of methoxyl groups of lignin may be primarily controlled by the δ^2H of precipitation and a Uniform fractionation with temperature. (Anhäuser et al 2016).

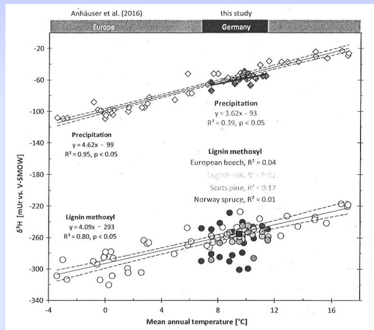

Fig. 4. Upper linear relationships: δ^2H_{precip} values versus MAT for the European north-south transect (white diamonds; Anhäuser et al., 2016) and Germany (blue diamonds). Lower linear relationships: δ^2H_{LM} values versus MAT for the European north-south transect (white circles; Anhäuser et al., 2016) and the German tree sampling sites (colored circles) which show no significant spatial δ^2H_{LM}-MAT relationship for each tree species (p values ≥ 0.19). Black box shows the mean δ^2H_{LM} of all core samples (excluding Norway spruce). For clarity purposes standard deviations are not shown.

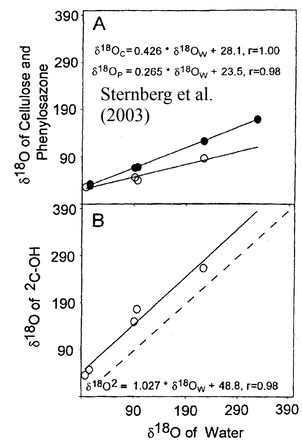

Fig. 3. A—$\delta^{18}O$ values of cellulose (full circles) and glucose phenylosazone (empty circles) versus the $\delta^{18}O$ values of water available during heterotrophically synthesized cellulose. One sample of glucose phenylosazone could not be recovered in sufficient quantities to analyze its oxygen isotope ratios. B—Calculated $\delta^{18}O$ values of the oxygen atoms attached to the second carbon of glucose moieties in the cellulose molecule versus the $\delta^{18}O$ value of the water available for heterotrophic cellulose synthesis. One extrapolated value of cellulose was used to calculate the $\delta^{18}O^2$ value of the seed culture having water with a $\delta^{18}O$ value of −1.45‰. Dashed line shows a relationship having a slope of 1 and intercept of 0.

- Glucose phenylosazone eliminates non-exchangeable oxygen and thus provides water source information.
- The study independently confirms the proportion of oxygen exchange (***fo*** = 0.42) with xylem water. (Sternberg et al. 2003; see also Sternberg et al. 2006, 2007).

Future directions (not a complete list)

- Fossil wood – longer records of climate change and correlation with other climate proxies (Epstein, 1995, Ward et al. 2005; Hunter et al. 2006, Jahren and Strenberg, 2008, Csank et al., 2011, Wolfe et al., 2012, Hook et al., 2015)
- Isotopes of other elements (^{15}N, ^{87}Sr, ^{44}Ca, Pb etc.) (Saurer et al., 2004; Drouet et al., 2005; Elhani et al. 2005; Hietz et al., 2010, Holmden and Belanger, 2010, Novak et al., 2010, Doucet et al., 2012, Hardtle et al., 2014, Miller et al., 2014)
- Other cellulose records – peat bogs, packrat middens (Pendall et al 1999; Hong et al. 2000; Zanazzi and Mora, 2005, Holzkamper et al., 2012, Zhu et al., 2014, Bramley-Alves et al., 2015)
- Humidity reconstruction (Edwards and Fritz, 1986; Pendall, 2000; Wright and Leavitt, 2006, Tsuji et al. 2008, Haupt et al., 2011, Munksgaard et al. 2017)
- Competition studies (Dawson et al. 1993, Moreno-Gutierrez et al, 2012)
- Air pollution studies (Saurer et al, 2004; Savard et al. 2005; Wagner and Wagner, 2006, Savard et al., 2009, Guerrieri et al., 2009, Rinne et al., 2010, Novak et al., 2010, Leonelli et al., 2012, Sensula 2016)
- Shifts in precipitation patterns – monsoon variation (Roden and Ehleringer 2006, Hartsough et al. 2008, Liu et al. 2008, Ballantyne et al., 2011, Managave et al., 2010, Schollaen et al., 2013 Hochreuther et al. 2016)
- Site specific analysis of isotopomers (Sternberg et al, 2003; 2008, Augusti et al. 2006; 2008)

Future directions (continued, still not a complete list)

- Water source, precipitation patterns (Treydte et al. 2006, Brienen et al., 2012, Williams et al. 2012, Rinne et al., 2013), soil water (Marshall and Monserud, 2006, Saurer et al., 2016)
- Fog water utilization (Dawson, 1998, Johnstone et al., 2014)
- Climate cycles and events – drought, ENSO (Wright et al., 1998; Saurer et al., 2000, Bale et al., 2011), Hurricanes (Miller et al. 2006, Li et al., 2011), Solar activity (Yamaguchi et al., 2010, Ogurtsov, et al., 2011, Prestes et al., 2014), Volcanic activity? (Tognetti et al., 2012)
- Mapping/modelling geographic variation in climate change (Saurer et al. 2002, Sidorova, et al., 2010, 2013, Porter et al., 2014, Keel, et al. 2016)
- Physiological responses (Brooks and Coulombe, 2009; Helliker and Richter 2008, Powers et al., 2009, Barnard et al., 2012, Fruse et al., 2012)
- Archaeological studies (Williams et al. 2005, Aguilera et al., 2011, Panyushkina et al., 2016)
- Tree stress and ecological interactions (Kress et al., 2009; Tene et al., 2011, Sarris et al, 2013, Jansen et al., 2013, Saffell et al., 2014, Marias, et al., 2014, Pflug et al., 2015)
- Annual growth analysis in trees without rings (Evans and Schrag, 2004, Ballantyne et al., 2011, Ohasi et al., 2015)
- Using isotopes for cross-dating (Roden, 2008)